Nanoscale

Volume 1 | Number 1 | Jan 2013 | Pages 1–100

Nanoscale

www.rsc.org/nanoscale

ROYAL SOCIETY OF CHEMISTRY

ROYAL SOCIETY OF CHEMISTRY

www.rsc.org/nanoscale

Journal Name

ARTICLE

Ru-core/Cu-shell bimetallic nanoparticles with controlled size formed in one-pot synthesis

I. Helgadottir[a,b], G. Freychet[a], P. Arquillière[a,b], M. Maret[c], P. Gergaud[a], P.H. Haumesser[a] and C.C. Santini[b]

Suspensions of bimetallic nanoparticles (NPs) of Ru and Cu have been synthesized by simultaneous decomposition of two organometallic compounds in an ionic liquid. These suspensions have been characterized by Anomalous Small-Angle X-ray Scattering (ASAXS) at energies slightly below Ru K-edge. It is found that the NPs adopt a Ru-core, Cu-shell structure, with constant Ru core diameter of 1.9 nm for all Ru:Cu compositions, while the Cu shell thickness increases with Cu content up to 0.9 nm. The formation of RuCuNPs thus proceeds through rapid decomposition of the Ru precursor into RuNPs of constant size followed by the reaction of the Cu precursor and agglomeration as a Cu shell. Thus, the different decomposition kinetics of precursors make possible the elaboration of core-shell NPs composed of two metals without chemical affinity.

Introduction

In order to meet the constant challenges of miniaturization in modern technologies, the manipulation of matter at the nano-scale becomes of crucial interest. For instance, metallic nanoparticles (NPs) are needed in a range of applications such as the fabrication of advanced microelectronic, magnetic or optical devices.[1-3] For this purpose, substantial effort has been focused on the formation of transition-metal nanoparticles by wet synthesis processes, using polymers, ligands and organic or inorganic templates. Unlike traditional solvents, ionic liquids (ILs) can be used to generate metallic NPs in the absence of any additive.[4,5] Ionic liquids are molten salts at room temperature, composed of an organic cation and an inorganic or organic anion. They are thermally and electrochemically stable, non-volatile and electrically conductive.

ILs behave like organic solvents, and can dissolve organometallic (OM) precursors. Interestingly enough, their decomposition in ILs leads to the precipitation of the metal under the form of metallic NPs, as was shown for the decomposition of a Ru OM precursor in imidazolium-based ILs.[6,7] Such process has provided stable suspensions of metallic NPs with accurate size control and high stability, without addition of any ligand.[8,9]

More interestingly, upon adding a copper precursor to the Ru solution, NPs were formed in a wide composition range with smaller sizes as compared to pure Ru or pure Cu prepared from a single precursor.[10] Such unexpected size reduction indicates some interaction between the two metals, which is quite surprising, considering that Cu and Ru are not miscible and

form no alloy.[11] In this article, we first summarize recent experimental results suggesting that the formation of RuCu bimetallic NPs proceeds through the rapid nucleation of Ru followed by the decomposition of CuMes on their surface. This mechanism is thus expected to lead to the formation of bimetallic NPs with a Ru core and a Cu shell. However, so far, no direct evidence of such a structure could be brought. Therefore, we now provide an experimental proof of the Ru core-Cu shell structure of the RuCuNPs using Anomalous Small Angle X-Ray Scattering (ASAXS) experiments. We can also explain the observed size evolution of these bimetallic NPs with Cu content as a result of their formation mechanism.

Ru, Cu and RuCu NPs in ionic liquids

Monometallic NPs

Previous studies have shown that the decomposition of $(\eta^4$-1,5-cyclooctadiene)$(\eta^6$-1,3,5-cyclooctatriene)ruthenium(0), [Ru(COD)(COT)] under H_2 at 0°C in 1-alkyl-3-methylimidazolium bistrifluoromethylsulphonylimide $(C_1C_nImNTf_2)$ yields RuNPs whose size increases from 1.1 to 2.3 nm as n increases from 4 to 8.[6,7] This size evolution could be related to a specific short-length order within the ILs, whose ions form a polar backbone carrying apolar alkyl ends. For intermediate alkyl chains (n=4 to 8), these apolar ends form discrete, isolated pockets in a polar matrix. The size of the RuNPs is comparable to and increases with the size of these apolar domains. Furthermore these suspensions are outstandingly stable, even at temperatures of 100°C. Such a stability is not only due to the confinement of RuNPs in the

non-polar domains of the structured IL but also to the presence of hydrides at the RuNP surface, [Ru]$_s$-H, as shown by *in situ* hydrogen-deuterium and spectroscopic experiments.[9,12]

The method was extended to the synthesis of CuNPs by the reduction of Mesitylcopper(I) (CuMes) under H$_2$.[13] This electrochemical reaction requires a higher temperature. Indeed, 5.1 nm crystalline zero-valent CuNPs can be readily formed at 100°C in C$_1$C$_4$ImNTf$_2$ (see Fig. 1, χ_{Cu}=1).[14] Under the same conditions, the decomposition of Ru(COD)(COT) provides RuNPs around 4 nm with broader size dispersion as compared to the synthesis at 0°C (see Fig. 1, χ_{Cu}=0). This effect can be attributed to a decrease of local order in IL together with a faster diffusion of the dissolved species.

Bimetallic RuCuNPs

By mixing both precursors in a 1:1 ratio, much smaller NPs (around 2.5 nm) are formed, with a remarkable narrow size distribution (±0.5 nm).[10] Other Ru:Cu compositions were systematically tested, according to:

$$\alpha[Ru(COD)(COT)] + \beta CuMes + xH_2$$
$$\rightarrow Ru_\alpha Cu_\beta + 2\alpha COA + \beta MesH \qquad \text{Eq. 1}$$
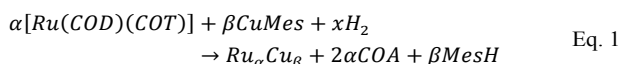
For this purpose, two solutions of 5x10^{-2} M [Ru(COD)(COT)] and of 5x10^{-2} M [CuMes] in [C$_1$C$_4$Im][NTf$_2$] were prepared and mixed with various molar fractions of Cu ($\chi_{Cu} = \beta/(\alpha+\beta)$) ranging from 0.005 to 0.995). The total metal concentration was kept at 5x10^{-2} M and α and β values were controlled by gas chromatography of the evolved by-products (cyclooctane (COA) and mesitylene (MesH)). From these experiments, it was observed that smaller NPs with narrower size distribution are formed in a wide range of Cu content in the mixture (χ_{Cu} ranging from 0.005 to 0.91, see white circles in Fig. 1).

Catalytic activity

A unique aspect in the synthesis of metallic NPs in ILs is that no additional ligand or stabilizer is needed.[4,8,9] As a result, the metal surface is accessible and active. This can be easily demonstrated by testing the catalytic properties of these NPs. For instance, the hydrogenation of benzene into cyclohexane is known to be catalysed by Ru. Therefore, the catalytic properties of RuNPs towards this reaction were tested at 150°C during 4 h under 0.9 MPa H$_2$ under 500 rpm. As expected, a conversion as high as 80% was obtained.

Conversely, under the same conditions, no reaction was observed with CuNPs. Interestingly enough, metallic NPs from RuCu mixtures exhibited a monotonous activity decrease as χ_{Cu} increased (the activity dropped to 6% at χ_{Cu}=0.93 (Fig. SI1).

Mechanism of formation of RuCuNPs

Several experiments were thus conducted to elucidate the mechanism of formation of these metallic NPs.[10,14] A first important observation is that the decomposition of Ru(COD)(COT) is much faster (several minutes) than the reduction of CuMes (several hours). Hence, the formation of

RuNPs is expected to occur before the reaction of CuMes with [Ru]$_s$-H.
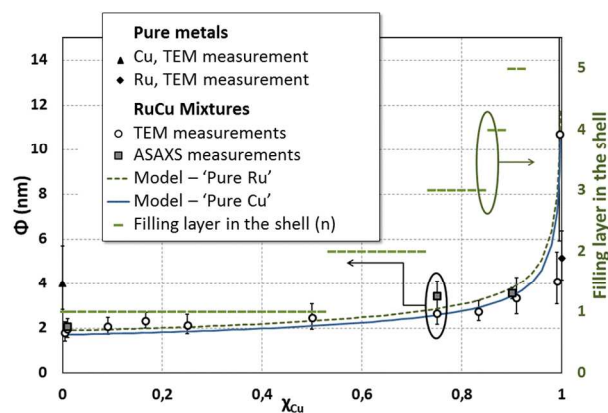
Fig. 1: Diameter evolution of the RuCuNPs with Cu content as measured by TEM (from ref 10) and ASAXS, and comparison with the model developed in the present work (with 147 atoms in the core). Mono- and bimetallic NPs were formed by decomposition of the OM precursors in C$_1$C$_4$ImNTf$_2$ for 4 h under 0.9 MPa H$_2$.

To verify this, the two reactions (formation of Ru nuclei and decomposition of CuMes) were performed successively. In a first experiment, a suspension of 2 nm RuNPs (formed in C$_1$C$_4$ImNTf$_2$ under H$_2$ at 25°C) was mixed with a solution of CuMes in the same IL and exposed to H$_2$ under 100°C for 4 h. After reaction, the diameter of the NPs increased from 2.0 to 2.5 nm, with Cu around Ru (as seen by Electron Energy Loss Spectroscopy, not shown here).[10] A second experiment was conducted using a suspension of RuNPs formed under D$_2$ (instead of H$_2$). In this case, the reaction of CuMes under argon released deuterated mesitylene. Finally, when Cu atoms were directly evaporated into a suspension of RuNPs in IL, distinct CuNPs were obtained, leaving the RuNPs unchanged.[15]

All these observations support the proposed mechanism, i.e. the reaction of CuMes with [Ru]$_s$-H. This reaction prevents further growth of RuNPs, stabilizing smaller NPs, even with a small amount of Cu (compare in Fig. 1 the points at χ_{Cu}=0 – pure Ru, black triangles, and χ_{Cu}<0.1 – mixtures with low Cu content, white circles). Another consequence is that the resulting bimetallic NPs do probably have a core-shell structure, with Ru in the core and Cu in the shell. To confirm this hypothesis, several characterisation techniques (HRTEM, EDX, XPS and Auger spectroscopy) have been used.[10] With HRTEM, only the crystalline structure of hexagonal close-packed Ru was detected, whereas EDX, XPS and Auger confirmed the presence of Cu within the NPs. Nevertheless, EELS experiments performed on RuCuNPs formed in two steps (*vide supra*) clearly indicated the presence of a Cu shell around a Ru core.[14] However, such structure has never been reported for RuCuNPs prepared in one step. The experimental evidence of such morphology is the main purpose of this work.

Materials and methods

Synthesis

1-butyl-3-methylimidazolium bistrifluoromethylsulphonylimide ($[C_1C_4Im][NTf_2]$) was used as an IL and synthesized from commercially available 1-methylimidazole, 1-butylchloride (Sigma Aldrich) and lithium bistrifluoromethylsulphonylimide (Solvionic).[16] (η^4-1,5-cyclooctadiene)(η^6-1,3,5-cyclooctatriene) ruthenium(0), [Ru(COD)(COT)], was synthesized from $RuCl_3$-$3H_2O$, 1,5-cyclooctadiene, methanol and zinc powder (Sigma Aldrich).[17] Mesitylcopper(I), [CuMes], (NanoMePS) was used without further purification.

Each precursor was dissolved in IL (dried overnight at 10^{-8} bar) under inert conditions and vigorous stirring to form a solution at 5×10^{-2} M. The two solutions were mixed together and stirred for 10 min in an autoclave under argon at room temperature, yielding a solution with a fixed total volume and the desired Ru:Cu molar ratio. The reactor was heated to 100°C under static vacuum. When temperature was stabilized, the solution was exposed to 0.9 MPa H_2 for 10 min. The autoclave was then sealed and maintained at 100°C for 4 hours yielding a black suspension containing metallic NPs. Gas chromatography (GC) analyses were performed with a HP 6890 GC system. For this purpose, aliquots of 0.25 mL of the solution containing NPs in IL were dissolved in 1.25 mL of acetonitrile in order to destroy interactions between mesitylene and cyclooctane with IL. Dodecane was used as internal standard in the solution.

Characterization

The NPs were observed by Transmission Electron Microscopy (TEM) using a Philips CM120 120 kV. For this purpose, the suspensions of NPs in IL were deposited on a TEM grid and dried. For each sample, a least 200 NPs were measured. Their size distribution was fitted by a lognormal law.

Anomalous Small-Angle X-ray Scattering (ASAXS) experiments were performed on the CRG-BM02 beam line at the European Synchrotron Radiation Facilities (ESRF), slightly below the Ru K-edge (22.117 keV). The vertical and horizontal dimensions of the focused beam were 100 and 150 μm, respectively. The suspensions of RuCu NPs in IL were contained in quartz capillaries of 1.5 mm diameter with wall thickness of 10 μm and sealed under argon. The capillaries were mounted perpendicularly on a multiple sample holder. The scattered intensities were detected with a FOC Roper Scientific CCD camera (1340x1300 pixels, 50 μm pixel size) at a sample-to-detector distance of 425 mm. The direct beam was stopped by a Pb disk of 2 mm diameter. The SAXS set-up was under primary vacuum except around the sample holder. A photomultiplier (PM) with a removable kapton foil placed just after the samples was used for both sample alignment and transmission measurements.

Results

Three suspensions with atomic fractions of Cu, χ_{Cu}, equal to 0.1, 0.75 and 0.9 as well as pure IL were measured at four energies, namely 21.6, 21.94, 22.06 and 22.1 keV. NPs with χ_{Cu}=0.1 are considered as pure Ru NPs whereas those with χ_{Cu}=0.75 and 0.9 are expected to be core-shell RuCuNPs.

Corrections for dark current and flatfield were applied. The SAXS intensities being isotropic, radial averaging over 360° was applied improving the level of precision. Fig. 2 shows the radial intensities measured for two capillaries containing pure IL and NPs dispersed in IL (χ_{Cu}=0.9). It appears clearly that below 3 nm^{-1} the intensity is dominated by the contribution of NPs whereas beyond this value the structure factor of IL is dominant with a first peak around 9 nm^{-1}.
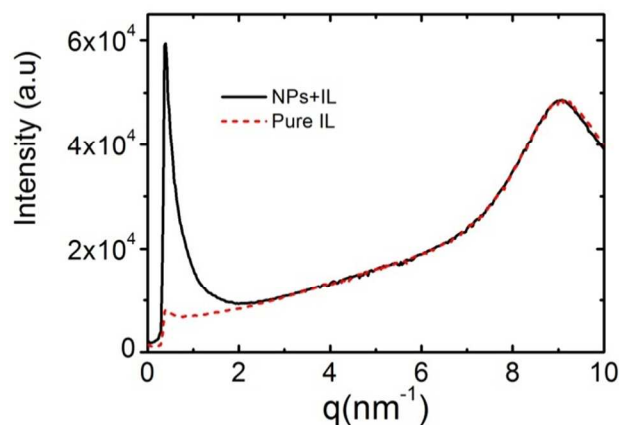
Fig. 2: Radial SAXS intensities as a function of the scattering vector, q, measured for the sample with χ_{Cu}=0.9 (black curve) and pure IL (red dashed curve) (E=22.1 keV, counting time=150 s).
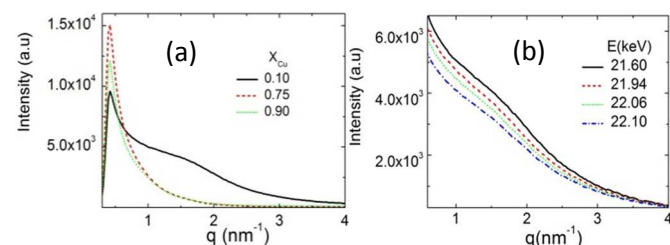
Fig. 3: (a) Change of the intrinsic scattering intensity of NPs, $I_{NP}(q)$, with the Cu atomic fraction at 22.10 keV. (b) Variation of $I_{NP}(q)$ with the photon energy (χ_{Cu}=0.1).

The intrinsic scattering intensities of NPs, $I_{NP}(q)$, were deduced from the total intensity, I_{IL+NP}, and the intensity of liquid, I_{IL}, corrected for sample transmission and monitoring (Fig. 3a). The decrease of $I_{NP}(q)$ with q is much faster for the Cu-rich NPs, as expected from the increase in size observed by TEM (Fig. 1). The peak around 0.4 nm^{-1}, which for χ_{Cu}=0.1 is well separated from the slower decrease starting from 0.8 nm^{-1}, can be attributed to larger particles, likely agglomerates of smaller RuCu NPs. Such agglomeration is quite important for χ_{Cu}=0.75. The variation of $I_{NP}(q)$ with the photon energy is shown in Fig. 3b for χ_{Cu}=0.1. The decrease of $I_{NP}(q)$ when approaching the Ru K-edge results from the decrease of the form factor of Ru atom, f_{Ru}; namely, f_{Ru} decreases from 40.7 to 37.4 by changing E from 21.6 to 22.1 keV, while the form factor of Cu, f_{Cu} remains around 29.2.

For bimetallic NPs, $I_{NP}(q,E)$ can be written as a function of the three partial structure factors, S_{ij} as follows:

$$I_{NP}(q,E) = \rho_{Ru}.\rho_{Ru}(E).S_{RuRu}(q)$$
$$+ (\rho_{Ru}(E).\rho_{Cu} + \rho_{Ru}(E).\rho_{Cu})S_{RuCu}(q)$$
$$+ \rho_{Cu}.\rho_{Cu}.S_{CuCu}(q) \qquad \text{Eq. 1}$$

where ρ_{Ru} and ρ_{Cu} are the electronic densities. [18] (Therefore, the differential intensity, $\Delta I_{NP}(q)=I_{NP}(q,E_1)-I_{NP}(q,E_2)$ is only dependent on $S_{RuRu}(q)$ and $S_{RuCu}(q)$ and its behaviour with q provides interesting information.[19] Fig. 4(a-c) shows the total intensities $I_{NP}(q)$ measured at 22.1 keV for the three Cu atomic fractions together with their corresponding differential intensities calculated between 21.6 and 22.1 keV after rescaling. It is striking that for $\chi_{Cu}=0.1$, $I_{NP}(q)$ and $\Delta I_{NP}(q)$ behave similarly, while for the two Cu-rich samples, the decrease of $\Delta I_{NP}(q)$ with q is much slower than the corresponding total intensities. This feature suggests strongly that Ru and Cu atoms in the nanoparticles are not randomly distributed. More precisely, the slower decrease of $\Delta I_{NP}(q)$ with q indicates that the Ru atoms are distributed in smaller volumes in agreement with a core-shell morphology where Ru and Cu atoms would occupy preferably the core and the shell of NPs, respectively. Furthermore, the three $\Delta I_{NP}(q)$ are really similar in the q-range [0.8-2 nm^{-1}], indicating a Ru core diameter almost identical in the three differently Cu enriched nanoparticles (Fig. 4d).

	ASAXS				TEM
χ_{Cu}	Φ (nm)	Φ_{core} (nm)	t_{shell} (nm)	NPs concentration (NPs/L)	Φ (nm)
0.10	2.06±0.07	1.9	-	$(1.1\pm0.3)10^{20}$	2.0±0.4
0.75	3.4±0.7	1.9	0.7	$(1.0\pm0.3)10^{19}$	2.7±0.6
0.90	3.6±0.3	1.9	0.79	$(2.0\pm0.3)10^{19}$	3.4±0.8

Based on such features, simulations of the intrinsic NPs intensities were done using the FitGISAXS program[20] allowing us to determine the diameter of the Ru core and the thickness of the Cu shell. Due to the strong contribution of the IL, the intrinsic intensities $I_{NP}(q)$ are very noisy above 3 nm^{-1} preventing any determination of the size dispersion. Therefore, for $\chi_{Cu}=0.1$, assuming a gaussian distribution of the Ru diameter with a full width at half maximum (FWHM) of 0.4 nm deduced from the TEM measurements, a value of 1.9 nm for the Ru core diameter was extracted, i.e very close to the TEM value (see Table 1). Above 0.8 nm^{-1} the corresponding simulated curve is in good agreement with the experimental one (Fig. 4a), since as already mentioned, below 0.8 nm^{-1} the strong increase of $I_{NP}(q)$ towards the smaller q-values comes from larger clusters.
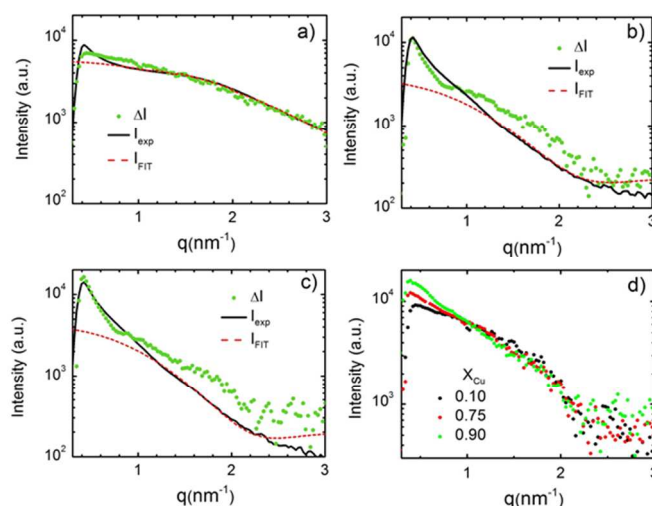
Fig. 4: Experimental (black solid line) and simulated (red dashed line) intensities obtained at 22.10 keV for (a) $\chi_{Cu}=0.1$, (b) $\chi_{Cu}=0.75$ and (c) $\chi_{Cu}=0.9$; the green points are the differential intensities, $I_{NP}(21.6keV)-I_{NP}(22.1keV)$, after rescaling with respect to $I_{NP}(q)$. (d) Comparison of the differential intensities obtained for the three compositions.

Table 1: Geometrical parameters of the RuCu nanoparticles deduced from the ASAXS and TEM measurements for the three compositions. Φ_{core} is the Ru core diameter, t_{shell} the Cu shell thickness, Φ the resulting total diameter of NPs and their concentration in the IL deduced from both ASAXS and TEM.

For the two other compositions, simulations were done keeping fixed the Ru core diameter at 1.9 nm and its gaussian distribution at 0.4 nm leading to a reliable determination of the shell thicknesses. All the parameters are given in Table 1 and compared to the TEM values. For $\chi_{Cu}=0.1$ and 0.9, the agreement is relatively good, while for $\chi_{Cu}=0.75$ the total diameter of NPs deduced from ASAXS equal to 3.4±0.7 nm is larger than, but still consistent with the value of 2.7±0.6 nm deduced by TEM. For this sample, the more pronounced agglomeration of NPs is probably responsible for the larger experimental error on the diameter measured by ASAXS.

From the transmission measurements and the values of the Ru core diameter and Cu shell thickness extracted from ASAXS, the concentrations of NPs in the IL could be deduced assuming that the atomic number densities of Ru and Cu in the core-shell particles are the ones of the pure metals and the molar density of IL remains unchanged in the presence of NPs. Again, for $\chi_{Cu}=0.1$ and 0.9, a good agreement between the values deduced from ASAXS and TEM is found. For $\chi_{Cu}=0.75$ the smaller density extracted from ASAXS could again be attributed to the more pronounced agglomeration of NPs.

Discussion

Based on the ASAXS extracted parameters and the proposed mechanism of RuCuNPs formation relying on the rapid nucleation of Ru followed by the agglomeration of Cu on the

Ru cores, the mean size and concentration of the bimetallic NPs can be estimated using rather simple structural description.

Let us assume that the metallic NPs adopt a nested icosahedral structure.[21] These icosahedral arrangements are composed of K layers of densely packed atoms (K=1 referring to the single central atom), contain $(10K^3-15K^2+11K-3)/3$ atoms and their successive layers are formed by $10K^2-20K+12$ atoms. For example, K=2 corresponds to the smallest icosahedron composed of a single layer of 12 atoms around the central atom. Each edge contains K atoms and has a length of approximately $2Ka_{at}$ (where a_{at} is the radius of atoms in the icosahedron, with $a_{Cu}=0.132$ nm and $a_{Ru}=0.146$ nm). Thus the volume of icosahedral clusters is given by:

$$V_{ico} = \frac{5}{12}(3+\sqrt{5})(2Ka_{at})^3 \qquad \text{Eq. 2}$$

The diameter of spherical NPs (Table 1) can be related to the volume of a specific icosahedral cluster composed of K layers, as follows:

$$\Phi_{ico} = \left(\frac{6V_{ico}}{\pi}\right)^{1/3} \qquad \text{Eq. 3}$$

The size evolution of bimetallic NPs with composition can thus be modelled assuming that:

1. The Ru precursor is first fully decomposed into Ru cores, whose size is the same for all particles where $0<\chi_{Cu}<1$, as suggested by ASAXS measurements. The number of Ru layers per core, K_{core}, is thus the only adjustable parameter in the model.
2. The particles grow by further decomposition of the Cu precursor, the shell being formed layer by layer.

Consequently, the bimetallic NPs are modelled by a core of N_{core} atoms of Ru (K_{core} layers), covered by n layers of Cu ($n\geq1$). Hence, these icosahedral NPs are formed of $K_{core}+n$ layers and contain $N_{core}+N_{shell}$ atoms. The latter numbers are related to the atomic fractions, assuming the total decomposition of both precursors (overall metal content was kept constant during the experiments):

$$N_{shell} = \frac{\chi_{Cu}}{1-\chi_{Cu}}N_{core} \qquad \text{Eq. 4}$$

Generally, the nth layer of the shell is only partially filled. In this situation, the number of Cu atoms in the shell is decomposed into:

$$N_{shell} = \left(\sum_{i=0}^{n-1} N_{shell,i}\right) + N_{shell,res} \qquad \text{Eq. 5}$$

where $N_{shell,res}\leq N_{shell,n}$. Based on these considerations, the diameter Φ can be interpolated by:

$$\Phi^3 = \frac{N_{shell,res}-N_{shell,n-1}}{N_{shell,n}-N_{shell,n-1}}(\Phi_n^3-\Phi_{n-1}^3) + \Phi_{n-1}^3 \qquad \text{Eq. 6}$$

At this stage, it is important to mention that the Φ_n values in Eq. 6 cannot be directly calculated from Eq. 3. Indeed, Cu atoms are significantly smaller than Ru atoms. Therefore, the Cu atoms in the shell layers are not expected to be densely packed. The diameter of the actual bimetallic NPs lies between two limiting cases:

1. The NPs are composed of a core of N_{core} Cu atoms, encapsulated with a shell composed of N_{shell} Cu atoms. This situation, referred to as "Pure Cu", underestimates the actual size of the NPs.
2. Conversely, the NPs are composed of a core of N_{core} Ru atoms, encapsulated with a shell composed of N_{shell} Ru atoms. This situation, referred to as "Pure Ru", overestimates the actual size of the NPs.

In both limiting cases, Eq. 3 can be used to compute Φ_n values, giving access to Φ by application of Eq. 6.

Before that, the number of Ru atoms in the cores, N_{core}, must be determined. This can be done by considering the Ru-rich end of Fig. 1. If one considers that in this region, the first layer of the shell is being progressively filled (which will be verified later), then size evolution may be described by Eq. 6 with n=1 in the "pure Ru" approximation:

$$\Phi^3 = \frac{N_{shell,res}}{N_{shell,1}}(\Phi_1^3-\Phi_{core}^3) + \Phi_{core}^3 \qquad \text{Eq. 7}$$

Therefore, Φ_{core} can be readily estimated by linear regression of the measured values of Φ^3 and extrapolation to $\chi_{Cu}=0$. Such an analysis was performed for $\chi_{Cu}\leq0.25$ and leads to $\Phi_{core}=1.9\pm0.3$ nm. This value is in excellent agreement with icosahedral clusters of 147 Ru atoms (corresponding to $K_{core}=4$ atomic layers of Ru), for which the theoretical diameter deduced from Eq. 3 is 1.88 nm. According to this result, the concentration of Ru cores in ionic liquid (and thus that of bimetallic NPs) decreases with the composition (χ_{Cu}) through:

$$[NPs] = \frac{[Ru]\mathcal{N}}{147} = \frac{(1-\chi_{Cu})[Metal]\mathcal{N}}{147} \qquad \text{Eq. 8}$$

where [Ru] and [Metal] are the Ru and total metal concentrations in mol.l^{-1}, respectively, and $\mathcal{N}$ is the Avogadro number.

It is now possible to plot the theoretical value of Φ upon the whole composition range for both limiting cases. These plots are compared to the experimental data in Fig. 1. Both limiting curves are close to each other, and are well matched with the experimental values. In particular, this simple model accounts

reasonably for the divergence of size observed for Cu-rich mixtures: all the available Cu atoms aggregate onto a limited number of Ru cores. Finally, it is worth noting that according to the model, in a wide composition range, the bimetallic NPs are composed of Ru cores covered with a partially filled monolayer of Cu atoms. Indeed, the first shell layer is filled for $\chi_{Cu} \approx 0.53$. This validates the composition range used to determine the size of the Ru cores ($\chi_{Cu} \leq 0.25$).

Finally, it is also possible to plot the theoretical evolution of the NPs concentration with their diameter, as both quantities are related to each other because total metal content is kept constant. This evolution can be compared with experimental ASAXS results, as this technique gives access to both the size and the concentration of the NPs (Table 1). Fig. 5 shows that experimental values are generally lower than the theoretical ones. This can be attributed to partial agglomeration of the NPs, which decreases the NPs concentration measured by ASAXS. Again, this effect is more pronounced for the sample with $\chi_{Cu}=0.75$.
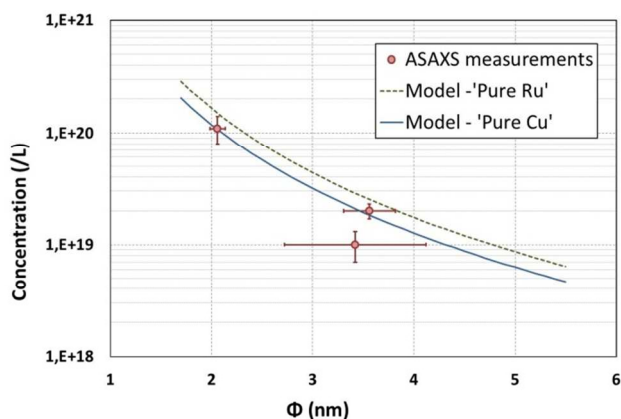
Fig. 5: NPs concentration dependence on size as predicted by metal mass balance (solid lines for "pure Ru" and "pure Cu" limiting cases, see text) and as measured by ASAXS.

Conclusions

Suspensions of bimetallic NPs of Ru and Cu have been synthesized by simultaneous decomposition of two organometallic compounds in an ionic liquid. These suspensions have been characterized by ASAXS at energies slightly below Ru edge. Careful examination of the intensity of the diffused X-ray at various energies allowed demonstrating that these NPs exhibit a Ru-core, Cu-shell structure. The diameter of the NPs was found to be in good agreement with the mean size measured by TEM. The diameter of Ru cores was estimated at 1.9 nm for all Ru:Cu compositions, the shell being thicker for larger Cu content in the mixture. All these results are well described by a simple model based on the mass balance between formation of Ru cores of constant size and subsequent agglomeration of Cu atoms onto them. These simple considerations account for the drastic increase of NP diameter observed for composition with excess Cu.

Along with previously reported results, this work unambiguously demonstrates that the formation of RuCuNPs by decomposition of Ru(COD)(COT) and Cu(Mes) in $C_1C_4ImNTf_2$ proceeds through the rapid decomposition of Ru(COD)(COT) into RuNPs of constant size followed by the reaction of CuMes with hydrides present on the Ru surface, $[Ru]_s$-H. This reaction initiates agglomeration of the Cu shell, but also blocks further growth of RuNPs, stabilizing in a wide composition range smaller NPs (with narrower size distribution) as compared to each metal separately.

Through the combination of differential kinetics (fast decomposition of Ru(COD)(COT), slow reduction of CuMes) and surface reaction, it is thus possible to form bimetallic NPs with core-shell structure using two metals that do not have chemical affinity.

Acknowledgements

Notes and references

[a] Univ. Grenoble Alpes, F-38000 Grenoble, France ; CEA, LETI, MINATEC Campus, F-38 054 Grenoble, France
[b] Université de Lyon, UMR 5265 CNRS-Université de Lyon 1-ESCPE Lyon, C2P2, ESCPE, 43 Boulevard du 11 Novembre 1918, 69616 Villeurbanne, France
[c] Univ. Grenoble Alpes, SIMaP, F-38000 Grenoble, France. CNRS, SIMAP F-38000 Grenoble, France

1. U. Caglar, V. Pekkanen, J. Valkama, P. Mansikkamaki and J. Pekkanen, C*eramic integration and joining technologies*, John Wiley, N.Y., 2011, 743-776.
2. H. Goesmann, C. Feldmann, *Angew. Chem. Int. Ed.* 2010, **49**, 1362,
3. D. Tsoukalas, *Int. J. Nanotech.*, 2009, **6**, 35-45.
4. J. Dupont, *Nanoparticles and catalysis*, Wiley-VCH, Weinheim, 2008.
5. J. Dupont, J. D. Scholten, *Chem. Soc. Rev.*, 2010, **39**, 1780-1804.
6. T. Gutel, J. Garcia-Anton, K. Pelzer, K. Philippot, C. C. Santini, Y. Chauvin, B. Chaudret and J.-M. Basset, *J. Mater. Chem.*, 2007, **17**, 3290-3292.
7. T. Gutel, C. C. Santini, K. Philippot, A. Padua, K. Pelzer, B. Chaudret, Y. Chauvin and J.-M. Basset, *J. Mater. Chem.*, 2009, **19**, 3624-3631.
8. P. S. Campbell, M. H. G. Prechtl, C. C. Santini and P.-H. Haumesser, *Curr. Org. Chem.*, 2013, **17**, 414-429.
9. P. S. Campbell, C. C. Santini, D. Bouchu, B. Fenet, K. Philippot, B. Chaudret, A. A. H. Padua and Y. Chauvin, *Phys. Chem. Chem. Phys.*, 2010, **12**, 4217-4223.
10. P. P. Arquilliere, I. S. Helgadottir, C. C. Santini, P.-H. Haumesser, M. Aouine, L. Massin and J.-L. Rousset, *Top. Catal.*, 2013, **56**, 1192-1198.
11. M. V. Raevskaya, I. E. Yanson, A. L. Tatarkina and I. G. Sokolova., *J. Less Common Met.*, 1987, **132**, 237.

12. T. Pery, K. Pelzer, G. Buntkowsky, K. Philippot, H.-H. Limbach and B. Chaudret, *ChemPhysChem*, 2005, **6**, 605-607.

13. C. Barriere, G. Alcaraz, O. Margeat, P. Fau, J. B. Quoirin, C. Anceau and B. Chaudret, *J. Mat. Chem.*, 2008, **18**, 3084-3086.

14. P. P. Arquillière, P.-H. Haumesser and C. C. Santini, *Microelectron. Eng.*, 2012, **92**, 149-151.

15. I. S. Helgadottir, P. P. Arquilliere, P. Brea, C. C. Santini, P. H. Haumesser, K. Richter, A. V. Mudring and M. Aouine, *Microelectron. Eng.*, 2013, **107**, 229-232.

16. L. Magna, Y. Chauvin, G. P. Niccolai and J.-M. Basset, *Organometallics*, 2003, **22**, 4418-4425.

17. P. Pertici and G. Vitulli, *Inorg. Syn.*, 1983, **22**, 176-181.

18. J.-P. Simon and O. Lyon, *Resonant Anomalous X-ray Scattering*, Elsevier Science, Amsterdam, 1994.

19. P. Andreazza, H. Khelfane, O. Lyon, C. Andreazza-Vignolle, A. Y. Ramos and M. Samah, *Eur. Phys. J. Special Topics*, 2010, **208**, 231-244.

20. D. Babonneau, *J. Appl. Cryst.*, 2010, **43**, 929

21. P. T. Martin, *Shells of Atoms*, Elsevier, Amsterdam, 1996.